

## Fundamental Studies on the Microwave Circuits and Electronics

Part II. Studies on Electronics of Microwave Planar Space  
Charge Tube with a Very Narrow Gap.

By

Nobuyoshi KATO and Toyosaku ISOBE

Department of Electronic Engineering

(Received October 15, 1957)

### Abstract

In this paper, calculation of the electronic admittance of a microwave planar diode in the shallow retarding field, experimental research of it and analytical study of mutual heating problem of thermal radiation among the electrodes of this tube are performed.

### Introduction and Synopsis.

In this paper, the studies of the gap phenomena of a microwave tube with a very narrow electrode spacing are performed.

In the first chapter\*, the approximate calculations of the electronic impedance of a diode with a comparatively weak retarding field and accordingly with a considerable strong effect of multi-velocity electrons are treated.

In the second chapter\*\*, the experimental studies of these phenomena are described.

The treatment in this chapter makes it possible to explain the physical meaning of the measured value of electronic admittance of a disc seal tube by arranging its position in such a way as the analysis made in Part I, chap. 2 is applicable.

In the third chapter\*\*\*, the thermal problems of the tube which has a very narrow spacing such as a disc seal tube are considered and the theoretical treatments of the effect of mutual heating by the thermal radiation. This phenomenon is essentially not a matter of electronics, but this problem is important from the stand point of high

---

\* This part was announced on the 30th Annual Joint Meeting of the three Institute of Electrical Engineers of Japan (May 1955).

\*\* This part was announced on the Meeting of the Microwave Research Committee (Sponsored by the Ministry of Education, Japan) No-2-15-43 (Conference of Feb. 1954).

\*\*\* This part was published on the Electrical Review of Japan, Vol. 38, No. 6 (Aug. 1950).

temperature engineering of a vacuum tube especially in the case when electrodes are very close to each other.

**Chapter 1. The Electronic Admittance of Microwave Diode in a Shallow Retarding Field.**

**1.1 Introduction**

The theoretical treatment of the high frequency electronic phenomenon occurring in a small spaced diode such as a remarkable effect of the velocity spread of the emitted electrons from the cathode is much complicated.

Therefore we are obliged to take approximate methods of analysis.

The authors extend Freeman's method<sup>1)</sup> to the case when the *d.c.* retarding field is not constant but varies directly as distance and *r.f.* field is superposed on the *d.c.* field as space constant.

This state has a close resemblance to a case that the potential of the plate is somewhat lower than that of the cathode and space charge effect appears slightly.

So the determination of the quadratic form of *d.c.* potential distribution is performed by referring to the exact form of the Langmuir's numerical solution of the distribution, and the operational condition of diode is limited to the assumption that the position of the potential minimum is on the anode surface.

**1.2 Theoretical calculation.**

In the following, it is assumed that the cathode and anode consist of two parallel planes sufficiently close so that the edge effect may be neglected.

We consider the electron motions in the field that negative *d.c.* voltage  $V_p$  and *r.f.* voltage  $V_a \cos(\omega t + \phi)$  are supplied on the anode of diode as shown in Fig. 1.1, where  $\phi$  is the phase angle of generator at the time of emission.

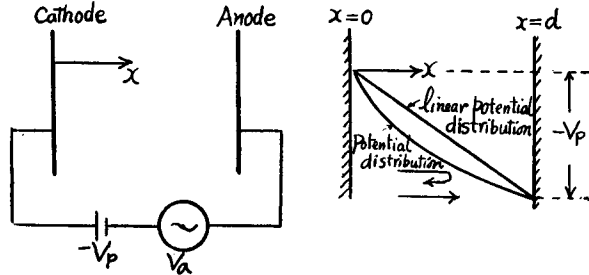


Fig. 1.1 Schematic of idealized diode.

As mentioned above, the *d.c.* potential distribution is approximated as following equation

$$-V_0(x) = Ax^2 + Bx \tag{1}$$

whose boundary values of anode is  $-V_p$ . Then the potential distribution in the space at any instant is

$$-V(x) = Ax^2 + Bx + \frac{x}{d} V_a \cos(\omega t + \phi) \tag{2}$$

and the electron trajectory in this space is determined by following equation

$$\ddot{x} = ax + b + c \cos(\omega t + \phi), \quad (3)$$

where

$$a = \frac{2eA}{m}, \quad b = \frac{eB}{m}, \quad c = \frac{eV_a}{md}$$

and  $e, m$  are charge, mass of an electron, respectively.

Solving Eq. (3) on the initial condition that is  $x=0, \dot{x}=v_0$  at the time  $t=t_0$ , we may obtain the following solutions.

$$\begin{aligned} x = & -\frac{b}{a} + \frac{1}{2} \left[ \frac{b}{a} + \frac{c}{\omega^2 + a} \cos(\omega t_0 + \phi) - \frac{1}{\sqrt{a}} \frac{c\omega}{(\omega^2 + a)} \sin(\omega t_0 + \phi) + \frac{v_0}{\sqrt{a}} \right] e^{\sqrt{a}(t-t_0)} \\ & + \frac{1}{2} \left[ \frac{b}{a} + \frac{c}{\omega^2 + a} \cos(\omega t_0 + \phi) + \frac{1}{\sqrt{a}} \frac{c\omega}{(\omega^2 + a)} \sin(\omega t_0 + \phi) - \frac{v_0}{\sqrt{a}} \right] e^{-\sqrt{a}(t-t_0)} \\ & - \frac{c}{\omega^2 + a} (\omega t + \phi). \end{aligned} \quad (4)$$

The transit time  $\tau_r$  of "returning" electron which has the too low initial velocity to reach the anode is the value of  $t-t_0$  (other than zero) which satisfies Eq. (4) for  $x=0$ .

Let  $\tau_r = \tau_{0r} + p\tau_1$ , as a first order approximation in  $p$  where  $p = V_a/V_p \ll 1$ .

Then

$$\tau_{0r} = \frac{1}{\sqrt{a}} \log \frac{1 - \frac{v_0 \sqrt{a}}{b}}{1 + \frac{v_0 \sqrt{a}}{b}} \quad (5)$$

and

$$\begin{aligned} \tau_1 = & \frac{eV_p}{2v_0 md(\omega^2 + a)} \left[ \left\{ \cos(\omega t_0 + \phi) - \frac{\omega}{\sqrt{a}} \sin(\omega t_0 + \phi) \right\} e^{\sqrt{a}\tau_{0r}} \right. \\ & \left. + \left\{ \cos(\omega t_0 + \phi) + \frac{\omega}{\sqrt{a}} \sin(\omega t_0 + \phi) \right\} e^{-\sqrt{a}\tau_{0r}} - 2 \cos(\omega\tau_{0r} + \omega t_0 + \phi) \right]. \end{aligned} \quad (6)$$

The transit time  $\tau_t$  of "traversing" electron which has the high initial velocity sufficient to reach the anode is the value of  $t-t_0$  which satisfies Eq. (4) for  $x=d$ .

Let  $\tau_t = \tau_{0t} + p\tau_2$ .

Then

$$\tau_{0t} = \frac{1}{\sqrt{a}} \log \frac{\left(1 + \frac{a}{b}d\right) - \sqrt{\left(1 + \frac{a}{b}d\right)^2 - 1 + v_0^2 \frac{a}{b^2}}}{1 + \frac{v_0 \sqrt{a}}{b}} \quad (7)$$

and

$$\begin{aligned} \tau_2 = & \frac{eV_p}{2F(v_0)md(\omega^2 + a)} \left[ \left\{ \cos(\omega t_0 + \phi) - \frac{\omega}{\sqrt{a}} \sin(\omega t_0 + \phi) \right\} e^{\sqrt{a}\tau_{0t}} \right. \\ & \left. + \left\{ \cos(\omega t_0 + \phi) + \frac{\omega}{\sqrt{a}} \sin(\omega t_0 + \phi) \right\} e^{-\sqrt{a}\tau_{0t}} \right. \\ & \left. - 2 \cos(\omega\tau_{0t} + \omega t_0 + \phi) \right], \end{aligned} \quad (8)$$

where

$$F(v_0) = \sqrt{d^2 + \frac{2db}{a} - \frac{v_0^2}{a}}$$

Fig. 1.2 shows the relation between  $-v_0 \frac{\sqrt{a}}{b}$  and  $\tau_0 \sqrt{a}$  parameter of which is  $-\frac{a}{b}d$ .

Then the total induced current is calculated by the following equation.

$$I(t) = -\frac{Ne}{d} \left[ \int_0^{v_m} f(v_0) \int_{t-\tau_r}^t \dot{x}(t, t_0) dt_0 dv_0 + \int_{v_m}^{\infty} f(v_0) \int_{t-\tau_t}^t \dot{x}(t, t_0) dt_0 dv_0 \right], \tag{9}$$

where

$$f(v_0) = \frac{mv_0}{kT} \exp\left(-\frac{mv_0^2}{2kT}\right), \quad v_m = \sqrt{\frac{-2eV_p}{m}}, \tag{10}$$

$K$ : Boltzman's constant,  $T$ : Absolute temperature of cathode,

$N$ : Number of electrons emitted per second.

The admittance calculated by the induced current is represented by the two terms as follows.

$$G_T = G_r + G_t, \quad B_T = B_r + B_t. \tag{11}$$

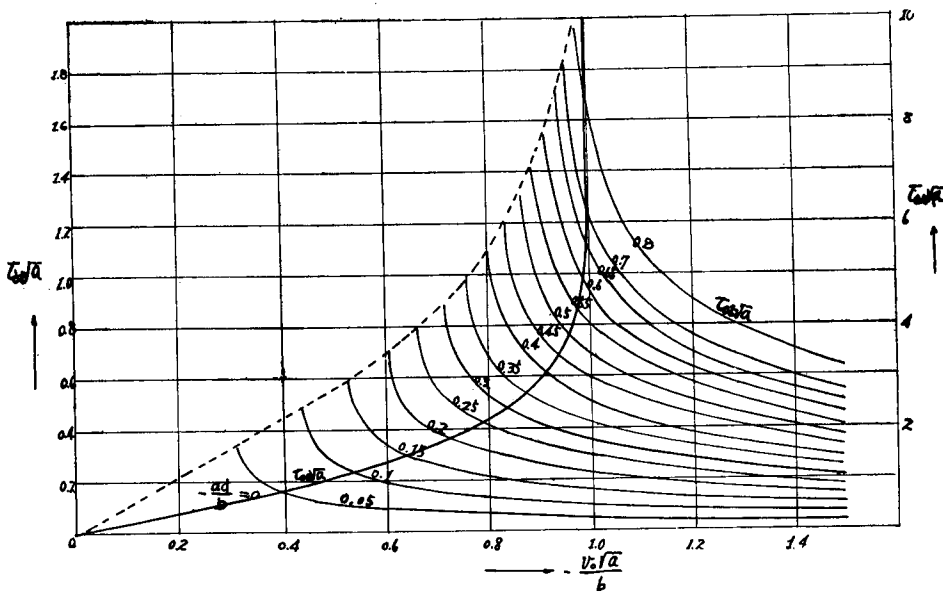


Fig. 1.2 The relations between  $-v_0 \frac{\sqrt{a}}{b}$  and  $\tau_0 \sqrt{a}$  parameter of which is  $-\frac{a}{b}d$ .

Where  $G_T, B_T$  are conductance, susceptance contributed by total electrons and  $G_r, B_r$  are  $G_t, B_t$  are that they are contributed by "returning" and "traversing" electrons, respectively.

These are represented as follows, respectively, by the calculations.

$$\left. \begin{aligned} G_r &= -\frac{I_0}{kT} \frac{e}{\omega^2 d^2} \int_0^{v_m} v_0 \exp\left(-\frac{mv_0^2}{2kT}\right) g_r(\omega, \tau_r, a) dv_0 \\ B_r &= -\frac{I_0}{kT} \frac{e}{\omega^2 d^2} \int_0^{v_m} v_0 \exp\left(-\frac{mv_0^2}{2kT}\right) b_r(\omega, \tau_r, a) dv_0 \\ G_t &= -\frac{I_0}{kT} \frac{e}{\omega^2 d^2} \int_{v_m}^{\infty} v_0 \exp\left(-\frac{mv_0^2}{2kT}\right) g_t(\omega, \tau_t, a) dv_0 \\ B_t &= -\frac{I_0}{kT} \frac{e}{\omega^2 d^2} \int_{v_m}^{\infty} v_0 \exp\left(-\frac{mv_0^2}{2kT}\right) b_t(\omega, \tau_t, a) dv_0 \end{aligned} \right\} \quad (12)$$

where

$$I_0 = Ne$$

and the suffix  $r, t$  in the above equation mean the "returning", "traversing", respectively, and  $g, b$  are as follows.

$$\left. \begin{aligned} g(\omega, \tau, a) &= \frac{2 - 2 \cos \omega \tau \cosh \sqrt{a} \tau - \frac{\omega \tau}{\sqrt{a} \tau} \left(1 - \frac{a \tau^2}{\omega^2 \tau^2}\right) \sin \omega \tau \sinh \sqrt{a} \tau}{\left(1 + \frac{a \tau^2}{\omega^2 \tau^2}\right)^2} \\ b(\omega, \tau, a) &= \frac{-2 \sin \omega \tau \cosh \sqrt{a} \tau + \frac{\omega \tau}{\sqrt{a} \tau} \left(1 - \frac{a \tau^2}{\omega^2 \tau^2}\right) \cos \omega \tau \cosh \sqrt{a} \tau + \omega \tau \left(1 + \frac{a \tau^2}{\omega^2 \tau^2}\right)}{\left(1 + \frac{a \tau^2}{\omega^2 \tau^2}\right)^2} \end{aligned} \right\} \quad (13)$$

Each of above Eq. (13) means the element of conductance and susceptance of electron admittance contributed by an electron with velocity  $v_0$  in the retarding field obtained by Eq. (2).

The relations between  $g, b$  and  $\omega \tau$  parameter of which is  $\sqrt{a} \tau$  are shown in Fig. 1.3, 1.4. The value of parameter  $\sqrt{a} \tau = 0$  corresponds to that of the linear potential distribution obtained by Freeman.

### 1.3 Numerical Calculations and Discussions.

As the examples, we treat the cases of following condition whose potential distributions are calculated from Langmuir's table, by assuming the cathode absolute temperature  $T$  and saturation current density  $J_0$  and coefficients  $a$  and  $b$  of quadratic form which approximate to its potential distribution are determined.

Table 1.1

Case	$d$ cm	$T$ °K	$V_p$ volt	$J_0$ A/cm <sup>2</sup>	$a$ sec <sup>-2</sup>	$b$ cm/sec <sup>2</sup>
$a$	$6 \times 10^{-3}$	1000	-0.7	0.1	$2.552 \times 10^{15}$	$0.152 \times 10^{20}$
$b$	$6 \times 10^{-3}$	1160	-0.47	0.16	$3.147 \times 10^{15}$	$0.296 \times 10^{20}$
$c$	$4.5 \times 10^{-3}$	1000	-0.55	0.1	$2.643 \times 10^{15}$	$0.124 \times 10^{20}$
$d$	$4.5 \times 10^{-3}$	1160	-0.43	0.16	$3.597 \times 10^{15}$	$0.435 \times 10^{20}$

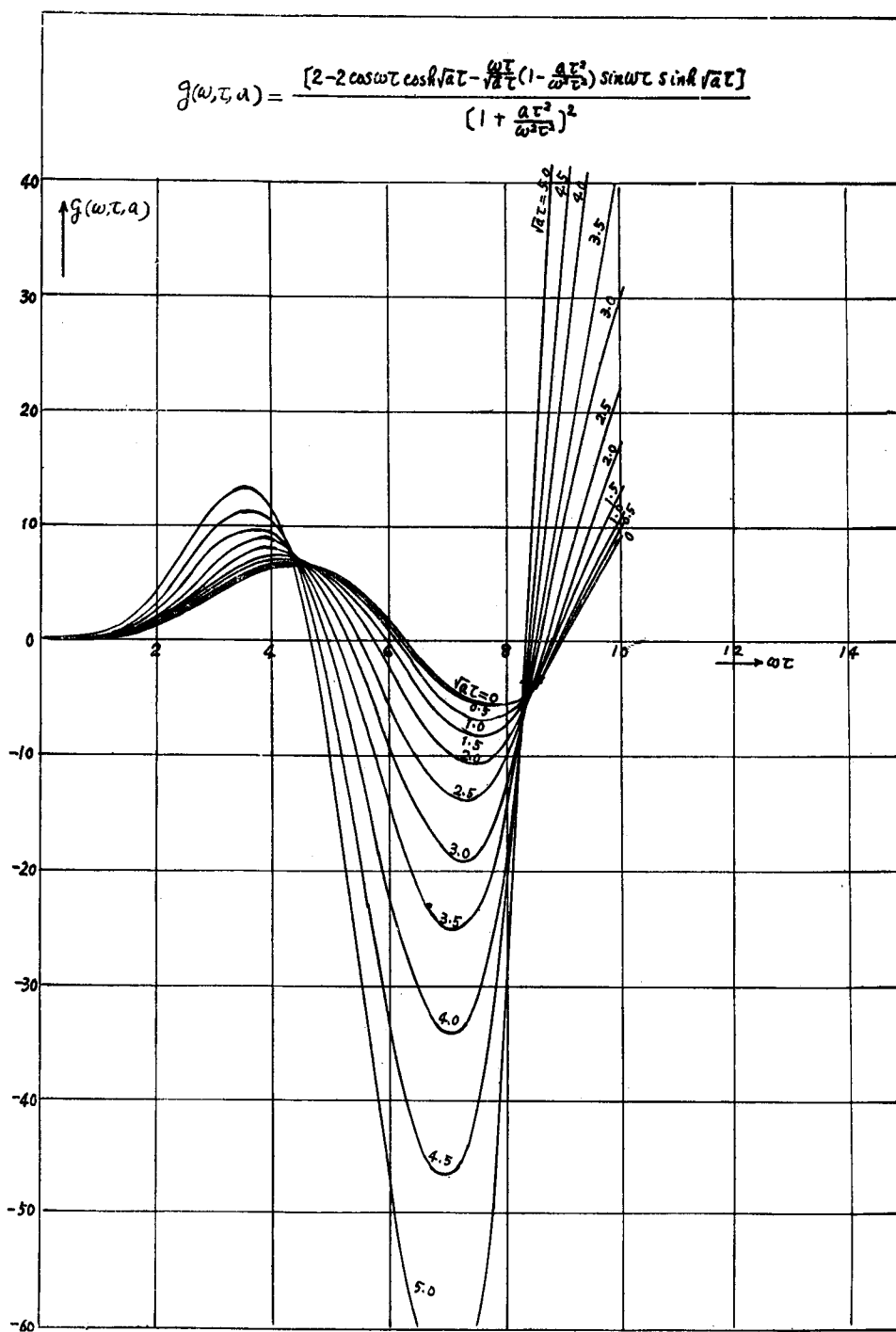


Fig. 1.3 The relation between  $g(\omega, \tau, a)$  and  $\omega \tau$  parameter of which is  $\sqrt{a} \tau$ .

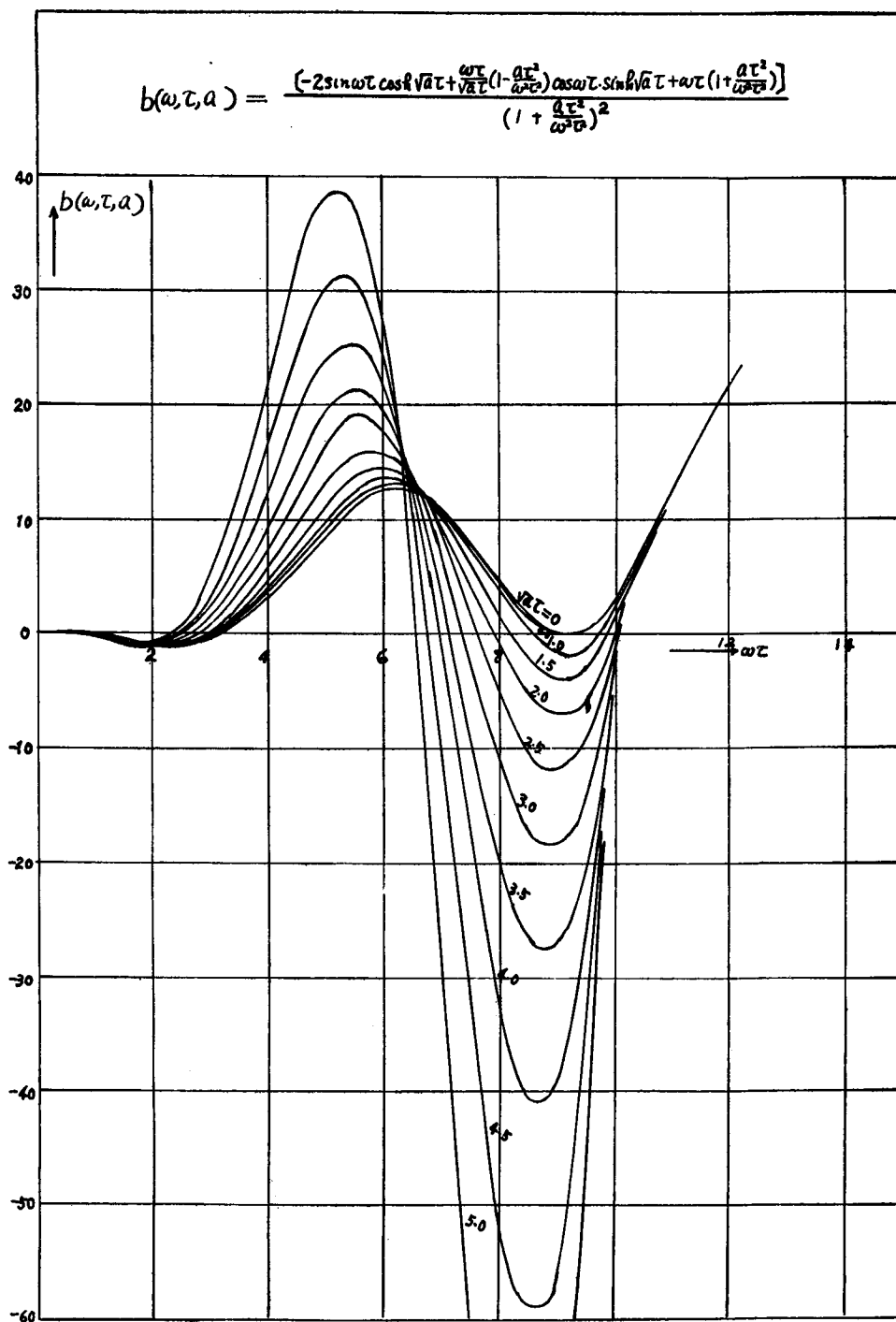


Fig. 1.4 The relation between  $b(\omega, \tau, a)$  and  $\omega\tau$  parameter of which is  $\sqrt{a}\tau$ .

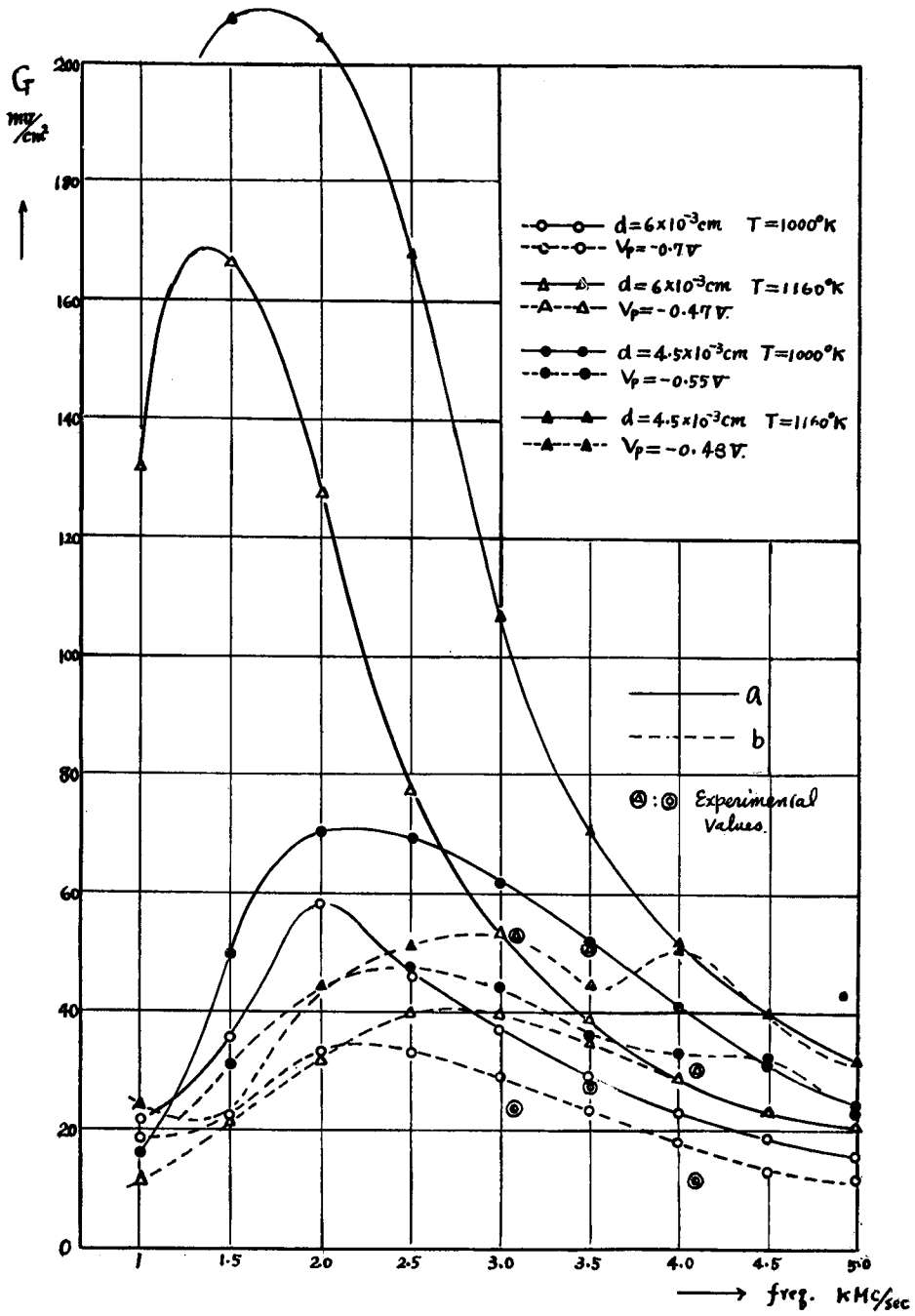


Fig. 1.5 Frequency characteristics of electronic conductance for different values of anode retarding voltage.  
 a): linear potential distribution b): quadratic potential distribution



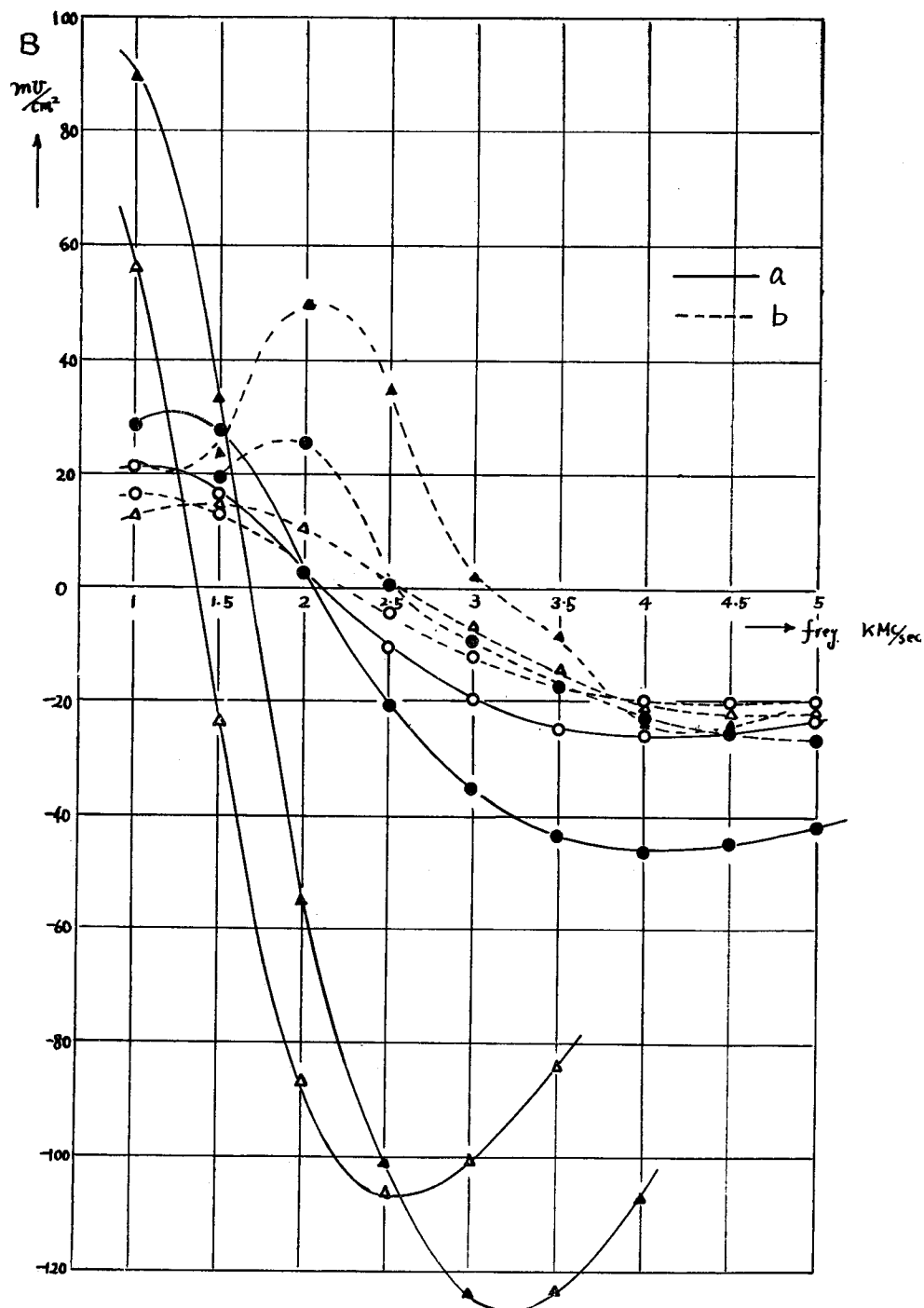


Fig. 1.6 Frequency characteristics of electronic susceptance for different values of anode retarding voltage.

Then calculating the frequency characteristics of  $G_T$  and  $B_T$ , we obtain the results as shown in Fig. 1.5 and Fig. 1.6. These results indicate the following characteristics;

- (1) The values of the electronic admittance in the case of the quadratic potential distribution in the gap are compressed compared with the case of the linear potential distribution and the closer gap we get, the larger this tendency becomes;
- (2) The peaks of conductances and the transition points of susceptances appeared in their frequency characteristics in the case that quadratic potential distribution situate higher frequency side than that of linear potential distribution on account of their transit time effects;
- (3) The rates of contributions by the "traversing" electrons to the electronic admittance calculated above are still negligible small compared with that of "returning" electrons.

In Fig. 1.5 some experimental values of the conductances corresponded to calculated values, which are obtained by the method described in next chapter are plotted in order to check the accuracy of our theoretical treatment.

## **Chapter 2. Experimental Studies on the Microwave Electronic Phenomenae of Electron Tube with very Close Electrode Spacing.**

### **2.1 Introduction**

In generally, for the measurement of electronic phenomena of microwave planar tubes, the method of measurement on the principle as customarily used that the gap admittance of the tube are regarded as a terminal load in the waveguide is adopted. The method described in this chapter is similar to that.

But in this measurement, the four-terminal network comes to be inevitably inserted between the reference plane of measurements and the electrode gap where the admittance under measurement lies. Then the key points of these measuring methods are what separating methods of electronic admittance from the measured normalizing admittance are taken in them.

A method to settle these points is to know previously the constants of the passive four terminal network which is inevitably inserted.

S. D. Robertson<sup>2)</sup> and T. Sekiguchi<sup>3)</sup> have obtained these constants by the purely experimental method.

The authors obtain these circuit constants by the purely theoretical calculation as described in Part I Chap. 2 by setting the tube as if its geometrical shape presented the post inserted in the guide. This treatment is somewhat primitive, but still has the more physical background than other methods.

**2.2 Principle of New Method.**

**2.2.1 Considerations as equivalent circuit.**

The schematic diagram of the measuring circuit is shown in Fig. 2.1. The wave guide of main part of measuring equipments is shortened the dimension of its height as if the shape of cathode electrode of tube inserted presented the state of post in the guide.

This wave guide is connected to standing wave detector,

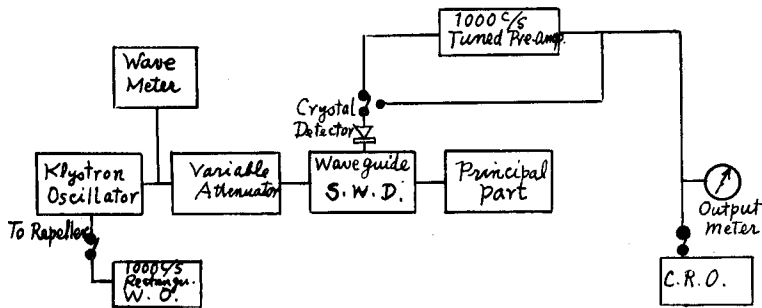


Fig. 2.1 Schematic Diagram of Measuring circuits.

by means of the tapered wave guide.

Fig. 2.2 shows the setting of tube in the main part.

Then the circuit problems arised are reduced to that treated in Part I chapter 2.

The equivalent circuit of this part is represented by the *T* type network as shown in Fig. 2.3(a).

We have represented the shunt element of this circuit  $Z_{12}$  by adding the supplemental term  $Z_{sup}$  to  $Z_{0r}$  the value of the case when the gap is closed, as shown in Fig. 2.3(b), where  $Z_{sup} = \frac{1}{QY_G}$ .

By the results obtained in the preceding Part I. Chapter 2. Eq. (37), the transformation coefficient *Q* of the impedance of gap capacity to its corresponding equivalent circuit value can be calculated.

If we know this value, we can obtain the absolute value

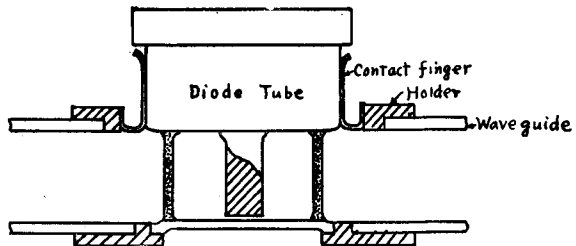


Fig. 2.2 Main part of measuring equipments with tube.

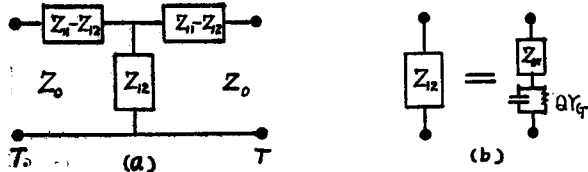


Fig. 2.3 Equivalent network of a tube under measurement.

of gap admittance by measuring the normalized admittance  $Z'_{12} = \frac{Z_{12}}{Z_0}$ .

Then we represent the gap admittance as follows by adding the gap susceptance to the value of electronic admittance  $Y_e$ .

$$Y_G = j\omega c + Y_e = G + jB = \frac{Y_0}{Q(Z'_{12} - \bar{Z}'_{12}) + \frac{Y_0}{j\omega c}} \quad (1)$$

where  $\bar{Z}'_{12}$  is the shunt value normalized by the characteristic impedance of the wave guide which is contained no electronic element and this value plays the basic part of measurement.

To obtain this, we must increase the negative grid bias of the tube until the indication of standing wave detector does not more vary. The shunt element value of this time is  $\bar{Z}'_{12}$ .  $Z'_{12}$  is the normalized admittance of the case electrons flow.

$Y_0$  is the characteristic admittance of the wave guide.

**2.2.2 Measurement of the Shunt Element Value.**

Choosing the reference plane of measurement for the plane of symmetry, we shall obtain its equivalent network as shown in Fig. 2.3. It is usually necessary the twice measurements of different position of short output plunger to obtain the value  $Z'_{12}$ .

But shifting the input and output planes of reference along certain distance  $D$  from the plane of symmetry, we can reduce this two pairs of terminal network to simple shunt element.

Then if we determine the distance  $D$ , the slunt element is obtained by only the once measurement.

Now, denoting the circuit parameters with regard to the initial reference plane as  $a, b, c$  and that to final planes of reference shifted by  $D$  as  $a', b', c'$  as shown in Fig. 2.4, we obtain the following relations among these parameters.

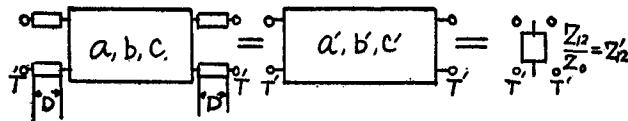


Fig. 2.4

$$\left. \begin{aligned} a' &= \frac{\sqrt{b+a^2}}{1-b} = \frac{Z'_{12}}{1 - (Z'_{11}{}^2 - Z'_{12}{}^2)} \approx Z'_{12} \\ b' &= 0 \quad a'/c' = 1 \\ D &= \frac{\lambda_g}{2\pi} \tan^{-1}(-a + \sqrt{b+a^2}) \\ a = c &= -jZ'_{11} \quad b = Z'_{11}{}^2 - Z'_{12}{}^2. \end{aligned} \right\} 4) \quad (2)$$

In addition to the method of above equation,  $D$  is easily obtained by experimental method such as measuring the distance between the contact point of 45° tangential

line to S curve of the post and its plane of symmetry as shown in Fig. 2.5.

Since the new planes of reference is determined, we obtain  $Z'_{12}$  by measuring the standing wave pattern on the input reference plane in case of output terminal makes open circuit by shorting plunger.

### 2.3 Experiments and Discussions.

Our experiments have been undertaken under the conditions of about below 0.3 mW level of input power to measure the electronic admittance in the state of small signal operation.

#### 2.3.1 Diode

Two tubes of 2C40 type diode such as the gap spacing  $d$  are  $45\mu$ ,  $60\mu$  have been measured. Fig. 2.6 shows the experimental results of gap admittance of a tube whose gap spacing is  $45\mu$ . Its heater voltage is 5.5V (d.c.).

The calculated values by the theories of Freeman and Sekiguchi are shown in it, for comparison. We assume its cathode temperature in this case is about  $900^\circ\text{K}$  by measuring the nature of initial current to plate voltage.

Fig. 2.7 shows the gap admittance of a tube of  $d=60\mu$ . Its heater voltage is 5.5V, or 6.5V. d.c.

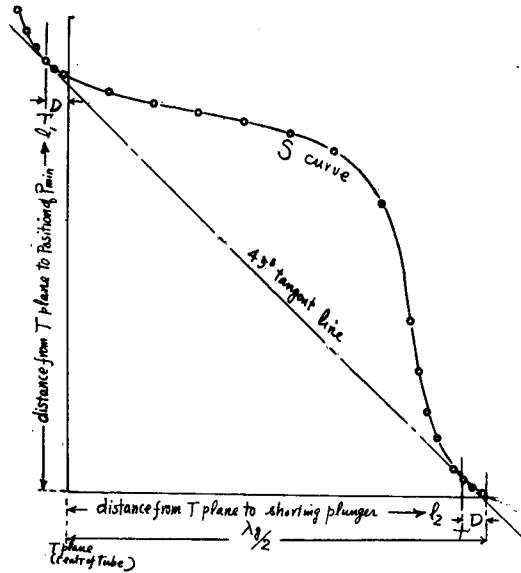


Fig. 2.5 An example of determination of distance by S curve method.

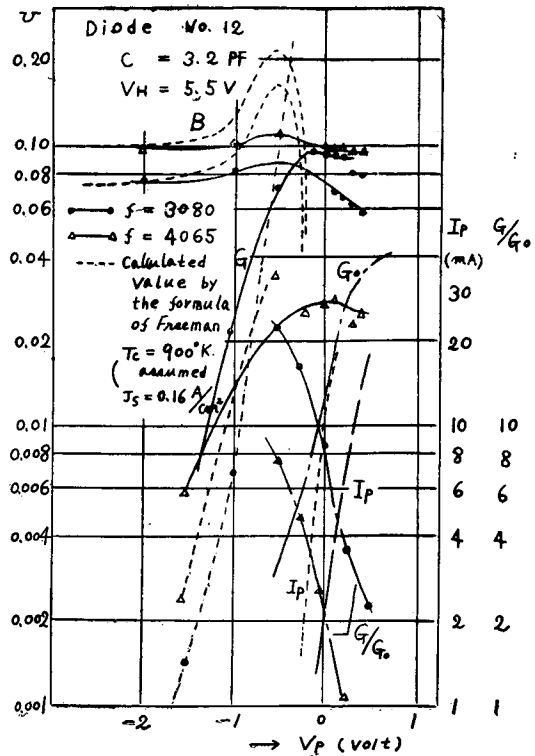


Fig. 2.6 Measured electronic admittance of diode ( $d=45\mu$ ) and comparison with theoretical values.

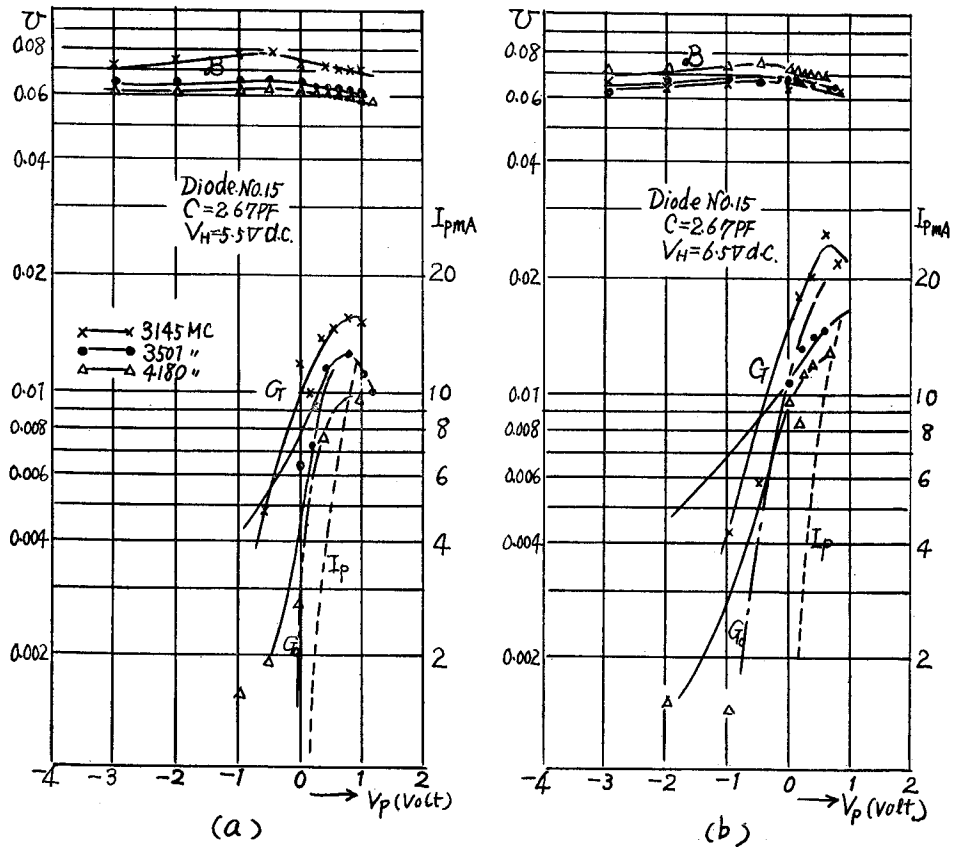


Fig. 2.7 Measured electronic admittance of diode ( $d=60\mu$ ).

The experimental values of this case are small as compared with their corresponding theoretical values. This is illustrated by the fact that the linear potential distribution does not occur in such an electrode spacing except the region of very deep negative potential of anode.

The comparison between the experimental values and the author's calculated values in the region of the potential distribution is quadratic form has been described in previous chapter.

We tested the tube with more close gap spacing as  $d=18\mu$  but we had to abandon this data by virtue of very poor emission of it.

### 2.3.2 Triode

On the correspondency between the input admittance of triode and gap admittance of diode, the network representation attended to the electron flow has been obtained by F. B. Llewellyn and L. C. Peterson<sup>5,6</sup>.

According to these results, the input admittance of triode corresponds to the

admittance of diode in the case of the tube which has very fine meshgrid.

The above conclusion on the basis of the "single velocity theory" are also applied to this case. Some experimental results of 2C40 type triodes which have no evaporation shield such as 446A are shown in the following. The setting of a tube in the wave guide is performed such as Fig. 2.8, that is the grid disc is set into the base of waveguide, and the disc with cooling fins put on the anode is set to contact the lower plane of waveguide through the thin micaplate in short circuited condition of output as far as the high frequency operations are concerned.

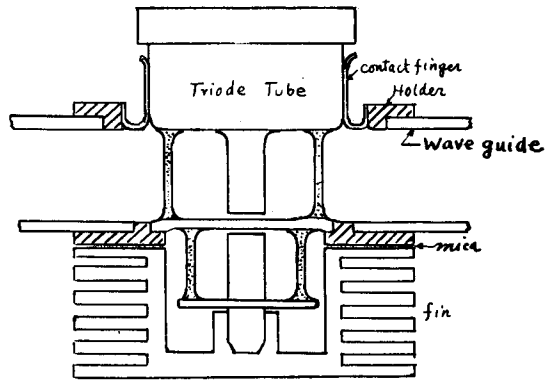


Fig. 2.8 Main part of measuring equipments with tube.

At first, we measure the input admittances of the tube on the condition of anode voltage is 200V constant and grid voltage can be varied from large negative value to positive one at the various frequencies.

As shown in Fig. 2.9 their natures show the similar characteristics to the case

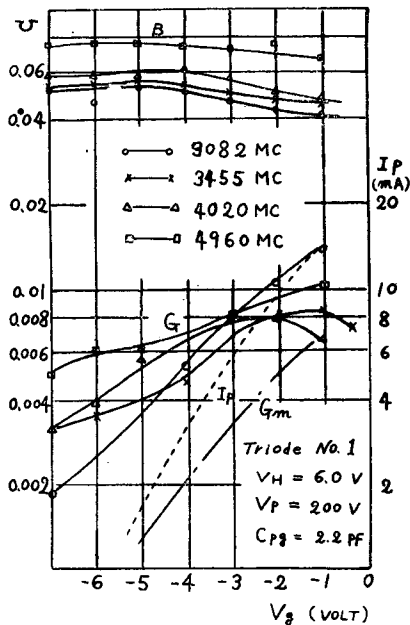


Fig. 2.9 The characteristics of input admittance of triode under the conditions of grid voltage varied.

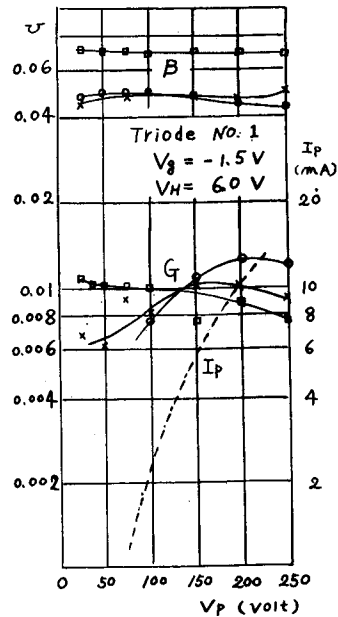


Fig. 2.10 The characteristics of admittance of triode under the condition of plate voltage varied.

of diode and it is recognized that the ratio of the effective conductance  $G$  to the  $G_m$  which corresponds to the *d.c.* admittance of diode declines rapidly as frequency increased.

Fig. 2.10 shows the results of measurement of input admittance at the condition of the grid voltage is  $-1.5V$  constant and anode voltage is varied.

From the preceding results compared the experimental value with theoretical one, about the diode and triode, we may conclude that the effects of returning electrons which have multivelocities appear in the electronic admittance of the tube of gap spacing which is the order up to  $60\mu$ .

### Chapter 3. The Problems of the Mutual Heating by Thermal Radiation among the Closed Gap Spacing of Electrodes such as Disc Seal Tube.

#### 3.1 Introduction

When the bodies whose proper temperature are very high are arranged closely in the vacuum, the each body repeats the absorption and reflection of energy of thermal radiations of each others, and its temperature of final state rises in somewhat than that of initial state.

This problem (so called the mutual heating of thermal radiation) is important to the case of microwave electron tube such as disc seal tube.

The authors will discuss about this problem of the case of parallel disc electrodes, and introduce the formula which represent its rising rate, and find especially the solution of this problem in the case of proper temperature of electrodes are distributed is resolved into that of the Fredholm integral equation of the 2nd kind.

#### 3.2 General Treatments

##### 3.2.1. The case of diode.

When we assume that the absorption coefficients of electrodes of diode I, II are  $A_1, A_2$  respectively, the reflection coefficients of them are represented  $(1-A_1), (1-A_2)$ , respectively.

Denoting the arriving rate of thermal radiation from electrode (I) to electrode (II) as  $\varphi_{12}$  and that from electrode (II) to electrode (I) as  $\varphi_{21}$  we obtain the following Table 3.1 about the quantities of thermal radiation of electrode (I) which go and return between electrodes (I) and (II).

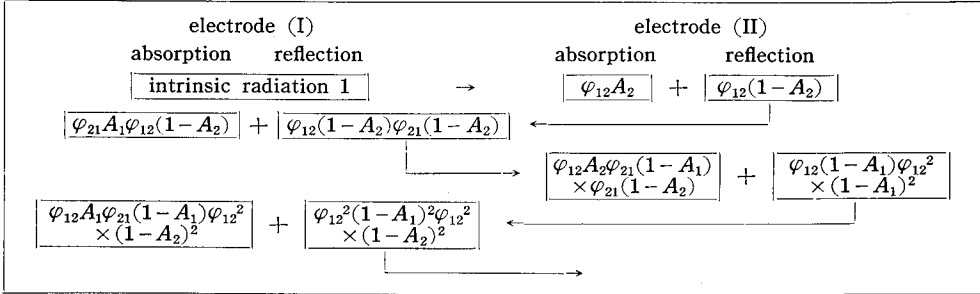
Again denoting the quantity of reabsorption of electrode (I) and quantity of absorption of electrode (II) of the thermal radiation energy from electrode (I) as  $\omega_{11}, \omega_{12}$ , respectively, we represent them as the following equations.

---

In the discussion of the frequency characteristics of this admittance, the effect of glass part is not negligible, but there is no any suitable method for separating it. We assume this effect by referencing the results in the preceding Part 1 chapter 2.



Table 3.1



$$\begin{aligned} \omega_{11} &= \varphi_{12}A_1\varphi_{12}(1-A_2) + \varphi_{21}A_1\varphi_{21}(1-A_1)\varphi_{12}^2(1-A_2)^2 + \dots \\ &= \frac{\varphi_{21}A_1\varphi_{12}(1-A_2)}{1 - \varphi_{12}(1-A_2)\varphi_{21}(1-A_1)} \end{aligned} \quad (1)$$

$$\begin{aligned} \omega_{12} &= \varphi_{12}A_2 + \varphi_{12}A_2\varphi_{21}(1-A_1)\varphi_{12}(1-A_2) + \dots \\ &= \frac{\varphi_{12}A_2}{1 - \varphi_{12}(1-A_2)\varphi_{21}(1-A_1)}. \end{aligned} \quad (2)$$

Similarly, denoting the quantity of absorption of electrode (I) and that of re-absorption of electrode (II) of the radiation energy from electrode (II) as  $\omega_{21}$ ,  $\omega_{22}$ , respectively, we represent

$$\omega_{21} = \frac{\varphi_{21}A_1}{1 - \varphi_{12}(1-A_2)\varphi_{21}(1-A_1)} \quad (3)$$

$$\omega_{22} = \frac{\varphi_{12}A_2\varphi_{21}(1-A_1)}{1 - \varphi_{12}(1-A_2)\varphi_{21}(1-A_1)}. \quad (4)$$

When we assume the temperatures of electrodes (I) and (II) at the thermal steady state are  $(T_1^\circ + \Delta T_1^\circ)$ ,  $(T_2^\circ + \Delta T_2^\circ)$  respectively, by mutual heating of thermal radiation, whose intrinsic temperatures are  $T_1^\circ\text{K}$ ,  $T_2^\circ\text{K}$  respectively, we obtain the following thermal equilibrium equations about each electrode as indicated in Fig. 3.1.

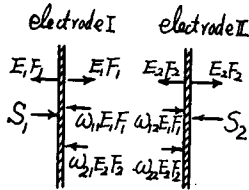


Fig. 3.1 Stationary state of thermal condition.

where  $E_1$ ,  $E_2$  are radiation energies per unit area in area of electrodes (I) and (II) respectively,  $F_1$ ,  $F_2$  are the half surface areas of electrodes, and  $S_1$ ,  $S_2$  are the impressed thermal quantities on electrodes (I) and (II), respectively.

The relations among the quantities of heat of each electrodes and those absolute temperatures are represented as follows.

$$\left. \begin{aligned} S_1 &= 2\sigma e_1 T_1^4 F_1 \\ S_2 &= 2\sigma e_2 T_2^4 F_2 \end{aligned} \right\} \quad (6)$$

and

$$\left. \begin{aligned} E_1 &= \sigma e_1 (T_1 + \Delta T_1)^4 = \sigma e_1 T_1^4 \left(1 + \frac{\Delta T_1}{T_1}\right)^4 \\ E_2 &= \sigma e_2 (T_2 + \Delta T_2)^4 = \sigma e_2 T_2^4 \left(1 + \frac{\Delta T_2}{T_2}\right)^4 \end{aligned} \right\} \quad (7)$$

where  $\sigma$  is emissivity,  $e_1, e_2$  are absorption coefficients of each electrodes.

Inserting Eqs. (6), (7) to Eq. (5) and rejecting higher powers of  $\frac{\Delta T}{T}$  than the first as  $T \gg \Delta T$ , we obtain the following equations about  $\frac{\Delta T_1}{T_1}$  and  $\frac{\Delta T_2}{T_2}$ .

$$\left. \begin{aligned} \frac{\Delta T_1}{T_1} &= \frac{1}{4\{(2-\omega_{11})(2-\omega_{22})-\omega_{12}\omega_{21}\}} \left[ \omega_{11}(2-\omega_{22}) + \omega_{12}\omega_{21} + 2\omega_{21} \frac{e_2 F_2 T_2^4}{e_1 F_1 T_1^4} \right] \\ \frac{\Delta T_2}{T_2} &= \frac{1}{4\{(2-\omega_{11})(2-\omega_{22})-\omega_{12}\omega_{21}\}} \left[ \omega_{22}(2-\omega_{11}) + \omega_{12}\omega_{21} + 2\omega_{12} \frac{e_1 F_1 T_1^4}{e_2 F_2 T_2^4} \right] \end{aligned} \right\} \quad (8)$$

Therefore, we can obtain the ascending rates of each electrode temperatures by Eq. (8) if we know each intrinsic temperature  $T_1, T_2$  and the values of  $\omega$ .

In order to know  $\omega$ , we must calculate the value of  $\varphi$ .

### 3.2.2 Definition of $\varphi$ .<sup>7)</sup>

The transfer of thermal radiation among the surfaces of any situation is calculated by the Lambert's cosine law, as far as rough surfaces are concerned. Considering the radiating surfaces as shown in Fig. 3.2. We may represent the transfer quantity of heat  $Q$  as follows.

$$Q = \varphi \sigma e_1 e_2 [T_1^4 - T_2^4] F_1 \quad (9)$$

$$\varphi = \frac{1}{\pi F_1} \int_{F_1} \int_{F_2} \frac{n_1 n_2}{S^4} dF_1 dF_2. \quad (10)$$

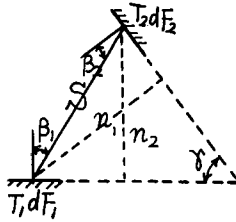


Fig. 3.2

Where  $S$  is the distance between the two surfaces,  $n_1, n_2$  are the length of perpendiculars which draw from  $dF_1$  or  $dF_2$  to the other surfaces in the plane containing these surfaces, respectively, and  $\beta_1, \beta_2$  are the angles between each normal lines and connecting lines  $S$ , respectively.

$\varphi$  is defined as the coefficient of solid angle. The solid angle looking from surface  $F_1$  into a certain point on the other surface  $F_2$ , which is denoted by  $\varphi'$  is expressed by following equation.

$$\varphi' = \int_{F_1} \frac{n_1 n_2}{\pi S^4} dF_1. \quad (11)$$

And by this equation, the distribution of the coefficient of solid angle on the surface  $F_2$  is obtained.

### 3.2.3 The Coefficient of Solid Angle between Two Parallel Discs<sup>7)</sup>.

We can calculate  $\varphi$  by the following way in the case that the two circular discs

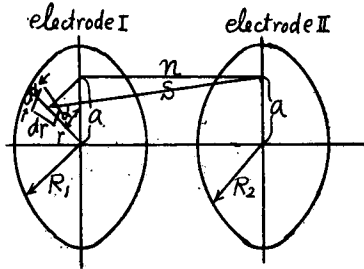


Fig. 3.3

are situated parallel to each other, coaxially as shown in Fig. 3.3.

$$\varphi = \frac{1}{2} \left[ \left( \frac{n}{R_1} \right)^2 + \left( \frac{R_2}{R_1} \right)^2 + 1 - \sqrt{\left\{ \left( \frac{n}{R_1} \right)^2 + \left( \frac{R_2}{R_1} \right)^2 + 1 \right\}^2 - 4 \left( \frac{R_2}{R_1} \right)^2} \right]. \quad (12)$$

If putting  $R_1=R_2=R$ ,  $\varphi$  is reduced to

$$\varphi = \frac{1}{2} \left[ \left( \frac{n}{R} \right)^2 + 1 - \frac{n}{R} \sqrt{\left( \frac{n}{R} \right)^2 + 4} \right]. \quad (13)$$

The relation between  $n/R$  and  $\varphi$  calculated by above equation as shown in Fig. 3.4. We can obtain the distribution of  $\varphi$  from electrode (I) to (II), that is  $\varphi'$ , in the process of calculation of Eq. (12), but here we omit this result and show only the relations among  $\varphi'$ ,  $n/R_1$  and  $a/R_1$  in Fig. 3.5.

### 3.3 Calculation of Temperature Distribution.

#### 3.3.1 Induction of Fundamental Equation.

In the preceding paragraph, we obtain the mean ascending temperature on the disc. But in practically it is important to know its temperature distribution.

In this section, we treat this problem on the assumption of  $R_1=R_2$  in Fig. 3.3 for simplicity. Now, assuming the distribution of thermal energy of disc (I) which in final steady state is  $E(r)$  and the intrinsic temperature distribution of disc (II) is constant on its surface on account of which has no impressed source and has room temperature, we represent  $d'Q'_{12}$  which is the transferred quantity of heat from disc (I) to disc (II) as follows.

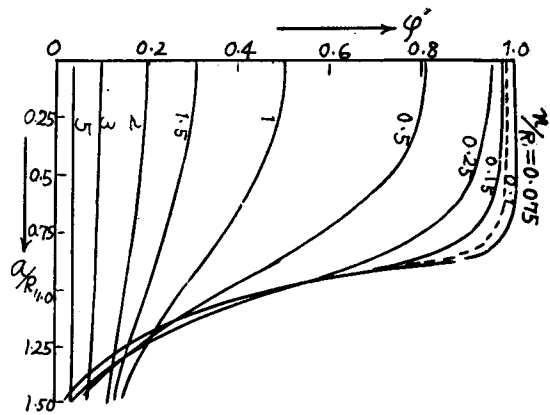


Fig. 3.4 Curve of  $n/R$  versus  $\varphi$ .

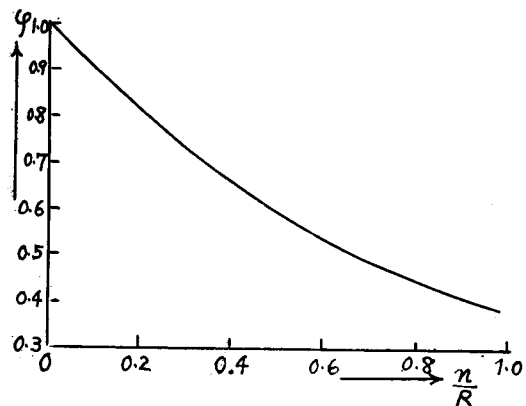


Fig. 3.5 Curves of  $\varphi'$  versus  $a/R$ , by taking  $n/R$  as a parameter.

$$d'Q_{12} = \frac{n^2}{\pi} \int_{F_1} E(r) \frac{1}{S^4} dF_1$$

where

$$S^2 = n^2 + a^2 + r^2 - 2ar \cos \alpha \quad dF_1 = r dr d\alpha$$

$$\therefore d'Q_{12} = \int_0^{R_1} E(r) K(a, r) dr \tag{14}$$

where

$$K(a, r) = \frac{2n^2 r (n^2 + a^2 + r^2)}{\left\{ (2^2 + a^2 + r^2) - 4(ar)^2 \right\}^{\frac{3}{2}}}$$

This quantity is the function of radius a of disc (II), and some of this quantity is transferred again to the point of disc (I) after it is absorbed somepart and the other is reflected.

Carrying out this process, we obtain the following Table 3.2.

Table 3.2

electrode (I)		electrode (II)	
absorption at certain point	reflection at certain point	absorption at certain point	reflection at certain point
radiation $E(r)$			
→		→	
$d'Q_{12R} A_1$		$d'Q_{12} = \int_0^{R_1} E(r) K(a, r) dr$	
$+ d'Q_{12R}(1-A_1)$		$\rightarrow d'Q_{12} A_2 + d'Q_{12}(1-A_1)$	
←		←	
$d'Q_{12R}$		$d'Q_{12R} = (1-A_2) \frac{n^2}{\pi} \int_{F_2} d'Q_{12} \frac{1}{S^4} dF_2$	
→		→	

The transferred quantity  $d'Q_{12R}$  to a certain point on disc (I) which is the reflected energy of the radiation  $E(r)$  of disc (I) from the disc (II) is as follows

$$d'Q_{12R} = (1-A_2) \frac{n^2}{\pi} \int_{F_2} d'Q_{12} \frac{1}{S^4} dF_2,$$

where

$$S^2 = n^2 + a^2 + \bar{r}^2 - 2a\bar{r} \cos \alpha' \quad dF_2 = a da d\alpha'$$

$\alpha'$ : angle between  $\alpha$  and  $r'$ .

$$\therefore d'Q_{12R} = (1-A_2) \int_0^{R_1} E(r) K_2(\bar{r}, r) dr, \tag{15}$$

where

$$\begin{aligned} K_2(\bar{r}, r) &= \int_0^{R_1} K(\bar{r}, a) K(a, r) da \\ &= \int_0^{R_1} \frac{4n^4 ar (n^2 + a^2 + \bar{r}^2) (n^2 + a^2 + r^2) da}{\left[ \left\{ (n^2 + a^2 + \bar{r}^2)^2 - 4(a\bar{r})^2 \right\} \left\{ (n^2 + a^2 + r^2)^2 - 4(ar)^2 \right\} \right]^{\frac{3}{2}}}. \end{aligned} \tag{16}$$

These processes are continued successively, but in practical case, the absorption coefficient of electrode (I) is very large on account of its oxide layer, etc. and that of electrode (II) is small.

Then we can treat these processes as one reflection process, approximately, and introduce its thermal equilibrium equation.

About electrode (I) as in Fig. 3.6, its absorption of energy are

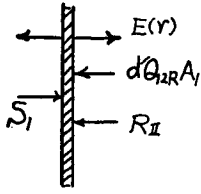


Fig. 3.6

- (1) reabsorption of the radiated energy  $E(r)$  of electrode (I),  $d'Q_{12}R A_1$ ,
- (2) absorption of the radiated energy from electrode (II),  $R_{II}$  and
- (3) the impressed thermal quantity  $S_I$ .

These quantities are in the state of equilibrium with its radiation  $E(r)$  on any point of electrode (I), that is

$$E(\bar{r}) = S_I + \frac{1}{2} A_1(1 - A_2) \int_0^{R_1} E(r) K_2(\bar{r}, r) dr + R_{II} \tag{17}$$

where  $S_I$  is the known function of radius of disc (I), and is represented as  $f(\bar{r})$ .  $R_{II}$  consists of the proper radiating quantity of electrode (II) and its reradiating that of absorption of  $E(r)$ . The former is very small comparing with the later, so  $R_{II}$  is represented by the later approximately. This is shown as follows

$$R_{II} = \kappa A_1 A_2 \int_0^{R_1} E(r) K_2(\bar{r}, r) dr.$$

Therefore, we rewrite Eq. (17) as follows.

$$E(\bar{r}) = f(\bar{r}) + \lambda \int_0^{R_1} E(r) K_2(\bar{r}, r) dr \tag{18}$$

where

$$\lambda = \frac{1}{2} A_1 [(1 - A_2) + \kappa A_2].$$

This is the Fredholm integral equation of the 2nd kind, and  $\kappa$  is assumed as  $\frac{1}{2}$  in this case.

### 3.3.2 Solving Method of Integral Equation.

Let us consider the nature of interative kern of integral equation shown in Eq. (16)

where,  $r$  is variable and  $\bar{r}$  is the certain point on electrode (I).

As integrating the right side of Eq. (16) numerically, first we fix a certain point of  $\bar{r}$  and some points or  $r$ , and integrate  $K(\bar{r}, a)$ ,  $K(a, r)$  by a about certain  $r$  from 0 to  $R_1$  then we obtain the characteristic curve of  $K_2(\bar{r}, r)$  to  $r$  of different fixed values of  $\bar{r}$ , as shown in Fig. 3.7.

Denoting these curve as  $K_2(\bar{r}_0, r)$ ,  $K_2(\bar{r}_1, r)$  we can represent them as the following Fourier series of sine generally.

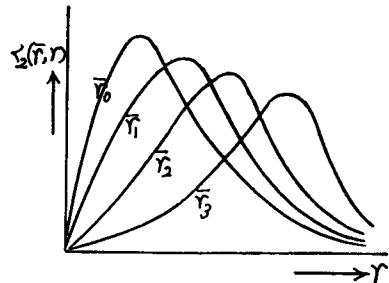


Fig. 3.7 Curves of  $K_2(r, \bar{r})$  versus  $r$ .

That is,

$$\left. \begin{aligned} K_2(\bar{r}_0, r) &= \sum_{m=1} A_{0m} \sin m\pi r \\ K_2(\bar{r}_1, r) &= \sum_{m=1} A_{1m} \sin m\pi r \\ \dots\dots\dots \end{aligned} \right\} \quad (19)$$

and assuming the distribution  $E(r)$  is axial symmetry, we can represent it as the following cosine series.

$$E(r) = x_0 + \sum_{n=1} x_{2n-1} \cos (2n-1) \frac{\pi}{2} r. \quad (20)$$

Then if the coefficients  $x_0, x_{2n-1} (n=1, 2, \dots)$  are known, the distribution are determined.

Now, in order to determine the  $(p+1)$  point values on the  $E(r)$ , we must calculate  $(p+1)$  terms of the series of Eq. (20).

When we define these coordinate points of  $\bar{r}$  as  $\bar{r}_0, \bar{r}_1, \dots, \bar{r}_p$  we obtain the following simultaneous equations, by inserting the relations of Eq. (19), (20) to Eq. (18) and putting the upper limet of integration  $R_1$  to unity.

$$\left. \begin{aligned} x_0 \left[ 1 - \lambda \sum_{m=1} \frac{A_{0m}}{m\pi} (1 \pm 1) \right] + \sum_{n=1}^p x_{2n-1} \left[ \cos (2n-1) \frac{\pi}{2} \bar{r}_0 - \lambda \sum_{m=1} A_{0m} F(m, n) \right] &= f(\bar{r}_0) \\ x_0 \left[ 1 - \lambda \sum_{m=1} \frac{A_{1m}}{m\pi} (1 \pm 1) \right] + \sum_{n=1}^p x_{2n-1} \left[ \cos (2n-1) \frac{\pi}{2} \bar{r}_1 - \lambda \sum_{m=1} A_{1m} F(m, n) \right] &= f(\bar{r}_1) \\ \dots\dots\dots \\ x_0 \left[ 1 - \lambda \sum_{m=1} \frac{A_{pm}}{m\pi} (1 \pm 1) \right] + \sum_{n=1}^p x_{2n-1} \left[ \cos (2n-1) \frac{\pi}{2} \bar{r}_p - \lambda \sum_{m=1} A_{pm} F(m, n) \right] &= f(\bar{r}_p). \end{aligned} \right\} \quad (21)$$

In the above equation, plus in the compound signs corresponds to the case of  $m$  is odd and minus to even, and

$$F(m, n) = \frac{1}{2 \left[ m\pi - \frac{(2n-1)\pi}{2} \right]} + \frac{1}{2 \left[ m\pi + \frac{(2n-1)\pi}{2} \right]}.$$

From Eq. (21), the unknown coefficients  $x_0, x_1 \dots x_{2p-1}$  can be obtained by determinant method.

From these coefficients, the distributions of  $E(r)$  is determined.

**3.3.3 Numerical Example.**

Let us calculate the distribution of  $E(\bar{r})$  as the case  $R_1=1, n/R_1=0.15, A_1=0.8$  and  $A_2=0.2$  and the radiation energy distribution of intrinsic temperature of electrode (cathode) I of disc seal tube is constant, unity and cosine distribution.

The results of calculations of the case that 4 points of  $\bar{r}$  are shown such as  $\bar{r}_0=0, \bar{r}_1=0.25, \bar{r}_2=0.5$  and  $\bar{r}_3=0.75$  are shown in Table 3.3 and Fig. 3.8.

Table 3.3

$f(\bar{r})$	$E(\bar{r})$
1	$1.212 + 0.364 \cos \frac{\pi}{2} \bar{r} - 0.050 \cos \frac{3\pi}{2} \bar{r} + 0.001 \cos \frac{5\pi}{2} \bar{r}$
$\cos \frac{\pi}{2} \bar{r}$	$0.013 + 1.450 \cos \frac{\pi}{2} \bar{r} - 0.010 \cos \frac{3\pi}{2} \bar{r} - 0.045 \cos \frac{5\pi}{2} \bar{r}$

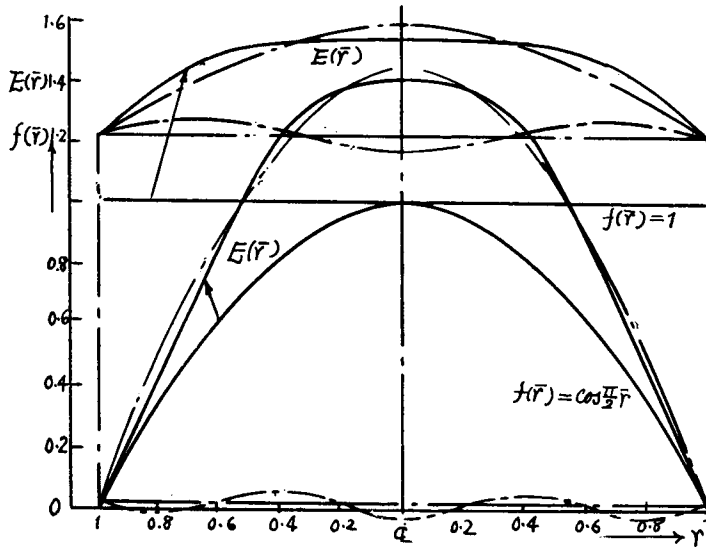


Fig. 3.8 Graphical representation of table 3.3.

By these results we inquire the tendency of more concentration of high temperature to the centre of electrode than the distribution of intrinsic temperature by the mutual heating.

This result is one example of calculation such as the distance of disc  $n$  is fixed constant. The charge of distribution of  $E(\bar{r})$  is wanted to know however, when  $n$  is varied, and similar numerical calculation about different value of  $n$  must be performed. This may be laborious work. But these characteristics can be conceived by considering that of  $\varphi'$  that was mentioned previously.

### Conclusions

In this part fundamental studies on microwave electronic phenomena of the tube which has a very narrow electrode spacing were treated.

The treatment of chapter 1, was done by the method of calculation of the total current in the external circuit induced by all electrons in the gap of diode at an arbitrary instant.

Comparing this result with that of a usual theory of linear retarding potential

distribution, we know the transit time effect on electronloading duing to space charge.

The principle of the measurement of chapter 2 are based on theoretical foundations developed in Part I Chapter 2, and this manipulation was simple.

So by measuring at many frequency points, we investigated the electron loading phenomena from the standpoint of its frequency characteristics. The results obtained agreed with the theoretical values in qualitatively.

Lastly, by the study of the tube from the stand point of high temperature engineering as treated in chapter 3, we know the thermal mechanism of the temperature rise of electrodes. These results are important for the design of the cathode.

Especially, the authors resolved the method of evaluating the temperature distribution of the electrode by the mutual heating of thermal radiation into the problem of solving the Fredholm integral equation of the second kind.

### **Acknowledgment**

The authors wish to thank Professor K. Maeda, Mr. M. Goto, Mr. K. Utagawa for their advances and encouragements in the course of the accomplishment of this work.

They are grateful to Mr. K. Takashima, Mr. T. Kitsuregawa and committee members of the Radiation Research Society of Japan and Mr. K. Imai for his assistantship of this work.

### **References**

- 1) J. J. Freeman: Joul. of Appl. Phys. Vol. 23, p. 743, 1952.
- 2) S. D. Robertson: B. S. T. J. Vol. 28, p. 647, 1949.
- 3) T. Sekiguchi: Joul. of the Faculty of Engineering, University of Tokyo. Vol. 24, No. 4, 1955.
- 4) Marcuvitz: Waveguide Handbook: Rad, L, Series 10. p. 125 (McGraw-Hill Book Co., Inc.)
- 5) F. B. Llewellyn and L. C. Peterson: Proc. I. R. E. p. 144 March 1944.
- 6) L. C. Peterson: B. S. T. J. Vol. 27, p. 593 1948.
- 7) T. Oga: The Transfer Theories of Heat and its Applications. (Iwanami Book Co., Inc.)